

AD-A063 023

WASHINGTON UNIV SEATTLE DEPT OF ATMOSPHERIC SCIENCES

F/G 8/12

ANNUAL REPORT NUMBER 10.(U)

DEC 78 N UNTERSTEINER, G MAYKUT, S MARTIN

N00014-76-C-0234

NL

UNCLASSIFIED

| OF |
ADA
063023



END
DATE
FILMED

3 -79
DDC

(13)

6

ANNUAL REPORT ~~NO. 10~~ Number 10.

15

CONTRACT ~~NO. 14-76-C-0234~~
NR 307-252

11

1 DECEMBER 1978

12

39p.

9

Interim rept.
1 Oct 77-30 Sep 78,

DDC
JAN 9 1979
F

DEPARTMENT OF ATMOSPHERIC SCIENCES
UNIVERSITY OF WASHINGTON
SEATTLE, WASHINGTON 98195

10

Norbert / Untersteiner,
Gary / Maykut,
Seelye / Martin,
Thomas / Grenfell
Peter / Kauffman

REPRODUCTION IN WHOLE OR IN PART IS
PERMITTED FOR ANY PURPOSE OF THE
UNITED STATES GOVERNMENT

This document has been approved
for public release and sale; its
distribution is unlimited.

DISTRIBUTION UNLIMITED

370 270

LB

CONTENTS

	Page
PERSONNEL	x
INTRODUCTION	1
DYNAMIC AND THERMODYNAMIC MODELING	3
Regional Heat Balance and Related Problems	3
Ice Forecasting	8
RADIATION IN ICE	12
Thin Ice Calculations	12
Laboratory Measurements	14
Scattering Experiments	17
Scanning Photometer	19
Optical Properties of Grease Ice and Cold Seasonal Ice	20
FLUID MECHANICS AND SEA ICE	23
Melting of a Vertical Ice Wall	24
Wave Damping by Grease Ice	24
REPORTS PUBLISHED AND IN PRESS	28
DOCUMENT CONTROL DATA - R & D	31
DISTRIBUTION LIST	32

ACCESSION		
NIS	Date	On <input checked="" type="checkbox"/>
DDC	Serial	<input type="checkbox"/>
		<input type="checkbox"/>
BY		
DISTRIBUTION/AVAILABILITY		
A		

PERSONNEL

The following scientific and technical personnel have been employed by the Contract during part or all of the period covered by this report:

DR. NORBERT UNTERSTEINER, Principal Investigator

DR. GARY MAYKUT, Co-Principal Investigator

DR. SEELYE MARTIN, Co-Principal Investigator

DR. THOMAS GRENFELL, Research Associate

MR. PETER KAUFFMAN, Electronics Technician

MR. DONALD K. PEROVICH, Predoctoral Associate

MR. EDWARD JOSBERGER, Predoctoral Associate

MR. DAVID HEDRICK, Predoctoral Associate (deceased October 1978)

MS. JANE BAUER, Predoctoral Associate (from July 1978)

INTRODUCTION

During the past year we concluded laboratory work on the optical properties of young sea ice and on the ablation of vertical ice walls submerged in warm sea water. Results from these two projects are being written up as thesis topics by Don Perovich and Edward Josberger, and should be available in report form in early 1979. A series of grease ice experiments were also carried out which have led to the derivation of an empirical damping equation for waves propagating into grease ice. Despite some equipment problems, laboratory measurements of light scattering by sea ice were continued. The results show that the phase function is quite sensitive to temperature, while the scattering coefficient appears to depend on the rate at which the ice was grown.

Field observations of ice growth were combined with our theoretical heat exchange, ice growth, and thickness distribution models to obtain estimates of: (i) the residence time of heat in the summer mixed layer in the central Arctic, and (ii) the magnitude of the oceanic heat flux in peripheral seas following ice formation in the fall. Other theoretical work included studies of: (i) the turbulent boundary layer adjacent to melting ice walls, (ii) the effects of snowfall pattern and date of formation on ice thickness and growth, (iii) year-to-year variability in the regional heat fluxes, (iv) the dependence of short-wave input to the polar oceans on ice and snow thickness, and (v) radiative transfer in young ice.

A field study of the temperature and salinity fields around a melting iceberg was carried out in the North Atlantic by Edward Josberger in cooperation with the International Ice Patrol. These observations will form part of Mr. Josberger's Ph.D. thesis. Also, as part of our instrument development program, we have almost finished construction of a new scanning photometer which will

allow the measurement of infrared albedos over polar ice and snow. Scientific results from previous work include papers on the optical properties of arctic ice and snow, energy exchange over young sea ice, large-scale heat and mass balance in the central Arctic, effects of ice thickness on the exchange of solar radiation, field and laboratory measurements of iceberg decay, a laboratory study of brine drainage features in young sea ice, and a field study of brine drainage in first-year ice.

DYNAMIC AND THERMODYNAMIC MODELING

Regional heat balance and related problems. Preliminary results of our large-scale heat exchange calculations were presented at the ICSI/AIDJEX Symposium on Sea Ice in a paper entitled, "Estimates of the Regional Heat and Mass Balance of the Ice Cover in the Central Arctic". This work incorporated our ice growth and thickness distribution models into a new regional averaging model. The calculations suggest that thermodynamic interactions between the Arctic Ocean and the atmosphere are much more vigorous than usually assumed; this is primarily a result of differential motions within the ice pack which cause the formation of leads. We found that areas of thin ice and open water make a major contribution to the overall turbulent heat exchange and salt flux to the mixed layer, while at the same time accounting for most of the net ice production and solar heat input to the upper ocean. A description of these results and related modeling work was prepared for publication in Naval Research Reviews. A paper on the energy exchange over young sea ice was also published in the Journal of Geophysical Research.

We have continued to analyze the regional results in an effort to clarify the effects of thickness variations on large-scale processes, and to identify areas where additional research is needed. In the two years (May 1962-May 1964) studied thus far, we found large year-to-year variations in the monthly and annual heat balance totals. These differences arose primarily from differences in ice strains. During October 1962, for example, the area being studied converged by about 16%, consuming most of the thin ice and open water; during the same period in 1963 there was a divergence of 12%, producing large amounts of open water. Somewhat smaller changes were noted during the other months.

Such large differences in the area of thin ice are naturally reflected in the regional flux totals. Whether either of these two years can be considered typical is not known. To determine long-term averages we will need to acquire strain records spanning many years. Satellite imagery and planned buoy arrays offer hope that such data will be forthcoming in the future.

The ice production estimates point up a second area where we need additional information. We found that during 1963 the net ice production in undeformed ice was equivalent to a layer some 80 cm in thickness covering the entire region. Some of this ice went into forming pressure ridges, while the rest went into replacing ice exported from the region. Unfortunately, we do not yet know enough about the ridging process or about ridge lifetimes to make confident estimates of how deformed ice contributes to the regional ice balance. In the coming year we plan to carry out numerical experiments designed to give us a better idea of the sensitivity of the regional mass balance to our ridged ice assumptions. A complete understanding of the problem, however, will not be possible until we learn more about keel decay and the processes associated with this decay.

Complicating the situation is the summer input of solar energy to the mixed layer through leads. Our figures show that (in the Central Arctic, at least) this energy source is probably somewhat larger than the heat input from the Atlantic layer. From the 1963 data we estimate that shortwave radiation absorbed in leads was sufficient to melt away about 13% of the ice pack in the Central Arctic - 3% by lateral melting on lead walls and 10% by melting on the underside of the ice. Melting at the upper surface decreased the amount of ice in the Basin by another 13%.

From these figures it appears that shortwave absorption in the ocean is at least as important to the mass balance as absorption by the ice itself. However, we do not clearly understand the details of the way in which heat absorbed in the ocean interacts with the ice. We suspect from the above evidence and from model calculations that the net effect of the energy absorbed beneath the ice is to enhance the rate of mass loss from the deformed ice. The energy is not necessarily concentrated at the keel bottoms, but more likely acts on small pieces of ice eroded from the keels. In a steady-state situation, net loss of deformed ice by export and melting must be balanced by ridge production. With this assumption and quantitative information on the melting process we should be able to obtain a rough check on predictions of ridging activity inferred from measured strain rates. We feel that keel ablation and its relation to absorbed shortwave radiation is knowledge crucial to making further progress in understanding the mass balance of the ice pack, and are presently working on the design of a field experiment to obtain this information. If a suitable field site can be located, we hope to carry out this experimental program during the summer and fall of 1980.

Recently we have carried out calculations aimed at determining the residence time of solar energy absorbed in the mixed layer. Theoretical calculations by T. Foster predict that heat carried into the mixed layer during the winter would be lost to the ice within 1-2 days, but it is not clear what happens during the summer when the surface layers of the ocean are strongly stratified. Heat and mass balance data from the AIDJEX experiment provided us with a new way to examine this problem. Growth rate measurements made at the main AIDJEX camp (Big Bear) during the summer of 1976 revealed several episodes of enhanced ablation which presumably correspond to periods

of divergence when more shortwave radiation was absorbed in the ocean. We therefore used strain observations and the thickness distribution model to calculate the average amount of open water in the region. We then weighted this by the incoming shortwave radiation to get an estimate of solar input to the ocean. Comparison of the two time series revealed a reasonably good correlation between periods of maximum ablation and maximum solar input. The relative magnitudes of these peaks, however, were not well correlated. During mid-August, for example, there was an extremely large increase in solar input, completely out of proportion to the corresponding peak in bottom ablation. From the strain data we had calculated that about 15% of the area should be open water, but an aerial mosaic showed that the open water was not distributed uniformly across the region - one corner contained 20-25% open water, while the area around Big Bear contained only 6-8%. Thus heat input near Big Bear was not typical of the area-wide average, demonstrating the difficulties involved in applying local measurements to regional problems. Nevertheless, divergence of the region as a whole should produce some corresponding increase in open water at Big Bear, and this is what the correlation in the maxima seems to show. The results from early July indicated a lag of 5-6 days between peak heat input and peak ablation; by August the lag had increased to 10-11 days. Heat entering the mixed layer during the summer thus appears to be retained several times longer than during the winter. Increasing stratification of the surface waters causes a continuing increase in residence time during the ablation season.

We have found from the regional calculations that a major contribution to the total annual ice production, turbulent heat loss, and salt flux is made during the fall when the summer leads refreeze. Our present treatment

79 01 08 053

assumes that the young ice is virtually snow-free, which is a reasonable assumption during the winter months, but which may be inadequate during the fall when snow accumulation is rapid. Because small amounts of snow can have a large effect on the heat and mass balance of young ice and because the fall is so important to the annual totals, we have begun a more detailed study of how snowfall affects regional heat exchange.

Our initial calculations were designed to see whether inclusion of the September-November snowfall would necessitate any basic changes in our thickness distribution model which assumes a one-to-one correspondence between growth rate and ice thickness. Specifying realistic air temperatures and snowfall rates during the fall, we ran a series of calculations with the thin ice model to learn how the time of initial ice formation influenced ice growth over a period of several months. We found that ice formed late in the fall grew to much greater thicknesses than ice formed early in the fall. Ice formed in September, for example, grew slowly due to relatively warm air temperatures and the rapid buildup of snow, while ice formed in November grew much faster in response to colder temperatures and a thin snow cover. Plotting contours of ice thickness vs. season and time of formation showed that ice forming at several different times could reach the same thickness on the same calendar date; the number of different formation times for which this can happen depended on how air temperature and snowfall varied with time. Interestingly, with smoothly decreasing temperatures and snowfall typical of the Central Arctic, we found that there are only two different formation times for a particular ice thickness. For example, on 1 November ice which is 50 cm in thickness could have formed either on 10 September or on 14 October. Oscillations in snowfall simulating periodic storms caused little change in this general pattern.

What these results mean is that there is not a one-to-one relationship between the thickness and growth rate (and hence the heat exchange) of young ice during the fall. Therefore, to take into account snowfall, some of the basic equations in the thickness distribution model will have to be reformulated. The overall effect will be to subdivide the thin ice categories according to their age (or snow depth). This would add another (undesirable) level of complexity to the model, but should be relatively straightforward to do. When modifications to the model are completed, we will repeat the regional calculations and assess the importance of snowfall. If snow accumulation on young ice proves to be a significant factor in the large-scale heat and mass balance, we will try to develop a simple parameterization of its effects for future applications. The fact that the thickness/growth rate dependence is only double-valued suggests that such a simplification may be feasible.

Ice forecasting. We have continued to improve and refine our simplified ice forecasting equations. Results from calculations with the thin ice model have been used to obtain appropriate values of coefficients in the turbulent heat parameterization and in the linearized longwave radiation term. Expressions for growth rates during the summer melt season have been developed. These expressions are suitable for inclusion directly into the ice thickness distribution model and are considerably easier to integrate than the thin ice model. However, the equations are still relatively complex and simpler forms would be desirable. While there seems to be no obvious way to simplify the equations without discarding important physics, some investigators (Bilello, Karelin) have reported a correlation between accumulated degree-days and the decrease in summer ice thickness. It seems unlikely, however, that such

correlations can be very general without explicitly taking into account incoming shortwave radiation. We plan to use the thin ice model and summer AIDJEX data to examine the relationship between these quantities in the hope of developing more generally applicable equations.

We believe on the basis of theoretical calculations that our ice forecasting equations adequately describe the winter growth of ice in refreezing leads, but must be modified before they can be used to describe seasonal ice growth in the peripheral seas. When compared with data from these areas, predicted ice growth is always greater than that actually observed. The reason must be due to some factor or factors which are neglected in the ice forecasts. Since shortwave fluxes are small during the fall freeze-up, the most likely factors are oceanic heat flux or snowfall. We therefore carried out a series of numerical experiments designed to see how large these quantities would have to be in order to obtain agreement between predictions and observations. We used Anderson's ice observations near Thule, Greenland as a basis of comparison. We found that, if there were no snow cover, the oceanic heat flux (F_w) would have to be over 100 cal/cm² day when the ice was very thin (10 cm), decreasing smoothly over a period of two months to a value of about 30 cal/cm² day by the time the ice had reached 80 cm in thickness. Comparison with data from the Russian Arctic indicated that even larger values of F_w would be required. Comparable values in the Central Arctic are 4 cal/cm² day. Changes in cloudiness produced a surprisingly large change in the results. Increasing the average cloud cover from 6/10 to 9/10 decreased the necessary F_w by 20-30%.

If there were no snow cover, total heat loss from the ocean during the growth period would have to have been about 5.5 kcal/cm². We do not have

simultaneous oceanographic and ice data with which to test the reasonableness of these results; however, an oceanographic station taken off West Greenland just before freeze-up suggests that the ocean would lose only about 2 kcal/cm² during the formation of 80 cm of ice. If this value also applies at Thule, then F_w would still have to be from 3-10 times larger (depending on ice thickness) than in the Central Arctic.

From these results it appears that, in addition to an F_w , some snow cover is required to explain the discrepancy between observed and predicted ice thicknesses. To place an upper limit on the amount of snow, we carried out another series of calculations including a snow cover, but requiring that F_w be zero. We found that the differences would be explained for the Thule data by a snow cover which increased continually throughout the observation period to a thickness of about 20 cm by the time the ice reached 80 cm in thickness. Anderson, however, states that there were no more than a "few" cm of snow during his observations, which would be in keeping with a fairly large oceanic heat flux in the region. Thus we see that reasonable values of snowfall and F_w provide a consistent explanation for the differences between observations and predictions. For this reason we feel that our forecasting equations can be applied in any region, but the particular form for a given location will depend on some general information regarding oceanic heat content and expected snowfall in the area.

Past efforts to measure F_w directly have been unsuccessful, while less direct methods based on temperature measurements within the ice have proved to be cumbersome. The calculations performed above suggest that rates of heat loss from the ocean can be determined in the marginal ice zone from a relatively simple data set without direct oceanic observations. As long as

the temperature profile within the ice remains reasonably linear, we can calculate the oceanic heat flux using our thin ice model (or forecasting equations) together with data on ice thickness, snowfall, air temperature and cloudiness. The method should work up to an ice thickness of 1 m and perhaps more, depending on how variable the air temperatures happen to be. In the following year we hope to have a data set from the Northwater area of Baffin Bay with which we can test this approach.

Another possible reason why predicted ice growth is larger than observed is that both the thin ice model and the forecasting equations ignore the change of internal heat content within the ice as it grows. Peter Schwerdtfeger has argued that this change can produce up to a 30% decrease in the expected ice growth. Although we are still reviewing his figures, crude calculations which we have carried out suggest no more than a 10-15% decrease. This is still a significant effect, particularly if we hope to use the thin ice model to obtain F_w as a residual. We are currently examining ways to include the change in heat content while retaining the basic simplicity of our models. Once a suitable method has been selected, we will carry out a series of numerical experiments to determine the importance of internal heat changes. If the effect of these changes is large enough to worry about, we will try to include a fairly precise treatment of it in the thin ice model. Exact treatment of internal heat may not be possible in the forecasting equations, however, and we may have to simulate the effect with empirical coefficients obtained from the results of the numerical experiments.

RADIATION IN ICE

A paper entitled "The Optical Properties of Ice and Snow in the Arctic Basin" was published in a recent issue of the Journal of Glaciology. The paper describes spectral albedos and extinction coefficients of thick first- and multiyear sea ice and snow, together with the application of these results to problems of radiative energy absorption, regional albedos, and remote sensing.

Thin ice calculations. In response to the need for more complete heat balance data on young ice, we have carried out a theoretical investigation of its interaction with solar radiation. A three layer model based on the work of Dunkle and Bevans was developed to treat radiative transfer between the thin snow and ice layers. The model includes a realistic lower boundary condition (namely that the upwelling irradiance must drop to zero at the bottom of the ice) and also takes into account the wavelength dependence of both the incident irradiance and the optical properties of ice. Although our laboratory studies indicate that the optical properties of young ice can be rather different from those of mature ice, we assumed that extinction coefficients in melting first-year ice provide a reasonable first approximation for thin ice.

Two distinct types of ice were considered. Of primary importance is young growing ice which occurs throughout the Arctic Basin during most of the year. Such ice has a high salinity, is relatively homogeneous, and is usually covered with dry windpacked snow. The second type, white ice, consists of a highly scattering granular surface layer above a thin transition zone and a consolidated lower layer. Although white ice does not constitute a major fraction of the thin ice during most of the year, substantial quantities can

be produced by summer ablation of first-year ice at the margin of the ice pack. White ice does not develop until the overlying snow layer has melted away.

Calculations of spectral and total transmission, absorption, and albedo were carried out for ice from 2-80 cm in thickness with up to 40 cm of snow cover. Energy absorption in the ice was sensitive to spectral albedos over the entire solar spectrum (roughly 400 to 3000 nm) as well as to the effects of cloudiness on the spectral composition of the incident irradiance. Since clouds remove essentially all the radiation beyond 1200 nm, total albedos for a particular ice type may vary by up to 30% depending on the degree of cloudiness. Radiative energy absorption is also sensitive to cloud cover, and on clear days it can be as much as 50 times larger in the upper 10 cm of the ice than on cloudy days. Below 10 cm most of the infrared has been removed and the energy absorption is about twice as large on clear days. In addition, total transmission to the ocean is 2 to 2.5 times as large under clear skies.

Depth profiles of net irradiance showed that for ice thinner than 40 cm an exponential law for the radiation field (Beer's law) is a poor approximation. Melting white ice, for example, can transmit up to 3 times as much energy to the ocean as Beer's law would predict. In order to incorporate the results of the present study into our thermodynamic ice growth model without using an involved radiation model, the albedo and transmission results have been parameterized as functions of snow and ice thickness. The results of the radiative calculations were submitted to the Journal of Glaciology under the title "The Effects of Ice Thickness on the Exchange of Solar Radiation over the Polar Oceans". The paper has been accepted for publication.

Laboratory measurements. Experiments on the optical properties of thin salty ice grown in the cylindrical freezing tank have been completed. The objective of the investigation was to study variations in the albedos and extinction coefficients of young ice in response to changes in ice thickness, growth rate, salinity, and temperature.

Eight experiments have been carried out and the data reduced. These include two runs with fresh water at -15°C air temperature, and six runs with saline water ($32 \text{ }^{\circ}/_{00}$ initial salinity) at air temperatures ranging from -10°C to -37°C . Two additional experiments with water of intermediate salinity ($16 \text{ }^{\circ}/_{00}$) at -10°C and -20°C have been completed and data reduction is in progress. Each run lasted from 10 to 15 days and included measurements of spectral albedos and transmission profiles as the ice developed. Concurrent measurements of the physical state of the ice included vertical temperature and salinity profiles, and ice thickness. After the ice growth was completed 12 cm cores were extracted and cut in half through a vertical plane. One-half of each core was stored for later use in the scattering measurements, and the rest was sectioned into thin vertical and horizontal slabs. Close-up photographs of these slabs were taken to study the bubble density profile and to show possible brine drainage features. Additional photographs in polarized light were used to delineate the crystal structure of the ice.

In each of the fresh ice experiments we were able to study both bubble-free and bubbly ice. Since the water was not initially saturated with air, the ice grew to about 80 mm before significant bubble nucleation took place. As the ice grew thicker, densely packed bubbles formed in long vertical columns rather than as discrete spheres as one finds for salty ice.

To the present limits of accuracy, the optical properties of bubble-free fresh ice are indistinguishable from those of pure water. As the bubbly layer grew, spectral albedos increased by only a few percent, and the total transmission decreased only slightly, indicating an extinction coefficient at 500 nm of less than 0.1 m^{-1} . Because the vertical sides of the columnar bubbles introduced very little backscattering, neither the albedo nor the attenuation was strongly affected even though the vapor volume was quite large. If the same vapor volume were distributed as a large number of spheres with about the same diameter as the cylinders, backscattering would be much larger. Thus, the fresh ice results are more representative of lake and river ice, and provide only a lower limit for the influence of bubbles on the optical properties of salty ice.

Albedos of salty ice increased much more rapidly with ice thickness than those of fresh ice. Actual values ranged from 0.4 to 0.9 depending on the ice temperature and initial growth rate. For example, the albedo at 500 nm of 25 cm ice grown at an air temperature of -10°C was 0.55, but when the ice was warmed to -2°C , the albedo decreased by 20%. In another run the ice surface was cooled below the eutectic temperature (-21°C) causing solid salt to crystallize out of the brine which formed a surface crust with an albedo similar to that of dry snow. Raising the surface temperature above -21°C caused the salt to redissolve, and the albedo dropped by about 30%.

Growth rate dependence was tested by comparing ice of the same thickness and temperature which was grown at air temperatures between -10°C and -36°C . Spectral albedos at all wavelengths were larger for ice which had grown faster. A difference of about 40% was observed between the extreme cases at all wavelengths.

Surprisingly, spectral albedos from the intermediate salinity (16 ‰) experiments were as much as 20% higher for a given growth temperature than for the corresponding high salinity (32 ‰) cases. This was caused by the formation on the surface of a thin brine skim at higher water salinity which was not present for intermediate salinity. The skim filled in surface irregularities and reduced backscattering in the uppermost ice layers. This effect was most pronounced for an air temperature of -20°C , while at T_{air} of -10°C the skim was barely noticeable, and albedos for the 16 ‰ and 32 ‰ cases were nearly the same.

In general, the spectral extinction coefficients (κ_{λ}) observed for growing young ice were from 1.5 to 15 times greater than for the thick ice studied during the melt season in our field experiments. Since the present results appear to be quite large, they have been checked by heating the ice with the artificial sun and determining the bulk extinction coefficients from changes in the vertical temperature profiles. Results from the two methods are consistent, supporting the accuracy of the optical data.

As with the spectral albedos, κ_{λ} is larger for higher growth rates. At 500 nm they ranged from about 2 m^{-1} , for ice grown at an air temperature of -10°C , to 12 m^{-1} for T_{air} of -37°C with the same initial water salinity. After the latter run the air temperature was raised to -20°C and the ice allowed to equilibrate. κ_{500} had decreased by about 6 m^{-1} . A further temperature increase to -2°C reduced κ_{500} by an additional 2 m^{-1} . The changes in extinction with temperature and growth rate appear to be smooth except when the upper layers of the ice cross the eutectic temperature.

Preliminary analysis indicates that extinction coefficients from both the intermediate and high salinity cases were about the same even though ice

salinities varied from about 4 ‰ to 14 ‰ in proportion to the water salinity. The growth rates, however, were nearly independent of salinity. In conjunction with the albedo results, this suggests that in the range 4 ‰ to 14 ‰ the optical properties of sea ice do not depend strongly on salinity, but that the initial growth rate and subsequent thermal history control the observed variations in the optical properties.

Final data interpretation is in progress using an adaptation of the radiative transfer model of Liou (1972) including surface refraction. This work is being carried out by D. Perovich for his M.S. thesis and should be finished during winter quarter. Mr. Perovich also presented some of his results at the Northwest Glaciologists conference in Vancouver, B. C. late last month.

Scattering experiments. Measurements of the light scattering properties of sea ice are currently in progress. To date we have completed 36 runs. We have been somewhat delayed by the failure of the laser's power supply, and it was necessary to use the old illumination system which required some improvements in the sample holder and light baffles. However, the laser has now been repaired by the manufacturer and is back in service. We expect the measurements to be completed in the next two months or so.

Light scattering is characterized by a coefficient, σ , which is the fraction of light scattered per unit length out of a collimated beam incident on the test sample, together with the angular distribution of the scattered radiation, the phase function. These two parameters specify the role of scattering in the transfer of radiation through sea ice.

For bubble free ice the scattering coefficient is on the order of $2 \times 10^{-6} \text{cm}^{-1}$ at 400 nm, and the phase function is nearly symmetric about an axis perpendicular to the incident beam. This indicates that the dominant process is Rayleigh scattering. Since the absorption coefficient is about 4×10^{-4} , scattering is negligible compared to absorption.

For salty ice the scattering is much more efficient; σ values measured so far lie between 0.07 and 0.3cm^{-1} . The phase functions show strong forward scattering and a minimum near 100° deflection angle with a slight increase for backscattering. Since the theoretical phase function for bubbles has a very weak backscattering component and a sharp drop near 90° (neither of which is found in our data), the influence of bubbles is probably small.

The phase function for both bubble free and salty ice is independent of wavelength from 400 nm to at least 800 nm. This indicates that the dominant scattering mechanism is controlled by the refractive indices of salt water, ice, and air, none of which are strongly wavelength dependent.

Substantial variations in the scattering coefficients and phase functions were observed for different samples. A strong temperature dependence between -10°C and -20°C was found; scattering coefficients for the colder samples were 2 to 3 times larger and the forward peak of the phase function was nearly an order of magnitude higher. Even larger variations were observed when the ice was cooled below the eutectic point and multiple scattering became significant.

Scattering coefficients for grease ice at -20°C were somewhat larger than for samples from the thin ice experiments at the same temperature and showed more side- and backscattering. This is reasonable since the grease ice is made up of many randomly oriented small crystals rather than a small number of large columnar crystals characteristic of the interior of the thin ice.

Results to date indicate that the shape of the phase function appears to depend on the current temperature of the sample while the scattering coefficient depends on the freezing rate. If this holds up, it will simplify the parameterization of the scattering properties for studying the bulk optical properties of the ice.

Attempts to grow bubble free salty ice using techniques suitable for fresh ice were unsuccessful. We will try degassing the water and growing ice in an atmosphere of helium which has a low solubility in water.

Scanning photometer. Construction of the scanning infrared photometer will be completed as soon as the electronics have been installed and the optical components aligned. The instrument is designed to scan visible and infrared wavelengths from 400 to 2500 nm using a circular variable interference filter together with a set of twelve fixed band interference filters. The spectral resolving power (wavelength \div bandpass) will range from 25 at 400 nm to about 50 at 1300 nm. Thus, in addition to extending the wavelength region we can observe, the new system will have almost 20 times higher spectral resolution between 800 and 1000 nm than do our present instruments. The radiation detectors will include a PbS photoconductor for the infrared beyond 1000 nm and a blue-enhanced, ultra-low-leakage photodiode for visible and near-infrared wavelengths. Initial estimates indicate that this system will detect spectral irradiances of less than $1 \mu\text{W}/\text{cm}^2/\text{nm}$ at all wavelengths - more than two orders of magnitude below the solar irradiance expected at 2.5μ on clear days in the Arctic.

The entire photometer is contained in an aluminum cylinder 20 cm in diameter and 20 cm tall weighing less than 35 pounds. To eliminate A.C. noise

problems, only D.C. powered components will be used together with rechargeable lead acid batteries. C-MOS electronics will be installed where possible for low power drain and low temperature operation.

The scanning photometer is intended primarily for measuring albedo and incident spectral irradiance, but it can be equipped with fiber optics if measurements within the ice are required.

Optical properties of grease ice and cold seasonal ice. Last year we participated in two joint experiments with Dr. Seelye Martin. The first, a laboratory study of grease ice and pancake ice grown in both fresh and salty water, was carried out in a 2 m wave tank using the profiling spectrophotometer. Spectral albedos and transmissions were measured at regular intervals as the ice grew. Ice density, temperature, and crystal structure were also observed concurrently.

Reduction of the optical data has been completed and interpretation is in progress. For ice grown in salt water, spectral albedos at 500 nm (α_{500}) increased from 0.038 for open water to 0.14 for 13 cm of ice when the growth phase was terminated. At longer wavelengths, the increase with ice thickness was less pronounced, but the spectral albedo curves for a particular thickness show a decrease from 500 to 1000 nm typical of ice and snow. At 1000 nm the albedo for 13 cm ice rose to 0.05, only slightly above the limit of specular reflection. The grease ice was allowed to freeze solid overnight, and another data set was taken. α_{500} then increased to 0.20 and α_{1000} to 0.084. The final ice thickness was about 12 cm due to consolidation of the platelets when the wave mixing stopped.

Extinction coefficients at 500 nm (κ_{500}) were initially on the order of 4 m^{-1} and showed a decrease of about 1.3 m^{-1} as the ice grew. After the ice had frozen solid, however, the extinction had increased by about 0.5 m^{-1} . The cause of these changes is not yet clear. The extinction coefficients are similar to those obtained from the thin ice experiments in cases where the growth rate was slow ($T_{\text{air}} = -10^\circ\text{C}$).

For the fresh ice, albedo increases with ice growth were only about 25% as large as for the salty ice and κ_{500} was also smaller (about 2.5 m^{-1}). Although the density of sea ice and fresh ice in the two runs was similar, the platelets in the sea ice were rougher around the margins and the index of refraction difference between ice and water was larger, giving rise to greater scattering efficiency.

The second experiment carried out in March 1977 was a field study of undeformed shorefast ice near Prudhoe Bay. This gave us the opportunity to measure the optical properties of cold seasonal ice together with the physical parameters influencing the scattering and absorption (salinity, temperature, crystal structure, and bubble density).

Albedos were rather large in comparison with those of warm summer ice especially at long wavelengths due to the very low brine volume in the upper layers. As a result the ice surface appeared bluish gray rather than blue. Surfaces covered with dry packed snow had very high albedos ranging from 0.8 to about 0.95 at 500 nm depending on solar elevation and surface roughness. The highest albedos were observed for smooth surfaces with the sun approximately 8 to 10° above the horizon.

Extinction coefficients of cold ice were larger than for summer ice - typically 1.5 m^{-1} at 500 nm as compared to between 0.8 and 1.2 m^{-1} . The

difference between the two was about the same at all wavelengths. Since the air temperature was usually between -25°C and -30°C , the surface temperature of the ice was often below the eutectic point and therefore the brine volume was nearly 0. In one case, however, the extinction coefficients were considerably lower ($\kappa_{500} = 0.85 \text{ m}^{-1}$). At this site the uppermost layers consisted of 5 cm of low salinity frazil ice over 11 cm of clear fresh ice, indicating that either flooding with fresh water or surface melting and brine drainage had occurred earlier in the season. Below 16 cm, however, the ice structure was essentially the same as in other areas. Clearly, the upper portions of the ice contribute significantly to the total transparency, and modifications in structure can have an important effect on the extinction coefficients of the entire layer.

Due to the tragic death of Mr. Dave Hedrick in October, we are spending additional time completing the scattering experiments while the freezing tank for our samples is still in operation. As a result publication of the results from the above experiments will be delayed until next year.

FLUID MECHANICS AND SEA ICE

During the past year, we wrote up four papers for publication; carried out laboratory studies on wave damping by grease ice and on the turbulent boundary layer adjacent to a vertical ice wall submerged in warm seawater; and carried out a cooperative field program in June 1978 with the International Ice Patrol on iceberg deterioration.

The published work consists of a paper by Edward Josberger titled "A Laboratory and Field Study of Iceberg Deterioration", with an Appendix by Martin, Josberger, and Kauffman on "Wave-Induced Heat Transfer to an Iceberg", both of which will be published in the Proceedings of the First International Conference on Iceberg Utilization. Second, we have rewritten Terren Niedrauer's Master's thesis which has been accepted by the Journal of Geophysical Research under the title "Brine Drainage Features in Young Sea Ice", by Niedrauer and Martin. Third, Edward Josberger with Steven Neshyba of Oregon State University have prepared a paper titled "An Estimation of Antarctic Iceberg Melt Rates", which was recently submitted in revised form to the Journal of Physical Oceanography. Fourth, S. Martin has submitted a paper titled "A Field Study of Brine Drainage and Oil Entrainment in First-Year Sea Ice" to the Journal of Glaciology. The writing up of this paper and some of the photographic processing, which stretched over two years, was partially supported by the Office of Naval Research and partially by the BLM/NOAA OCS program. Finally, the work by Martin and Kauffman on the interaction of grease ice and ocean waves was presented at the meeting of the Pacific Division of the AAAS on 15 June 1978 under the title "A Laboratory and Field Study of the Interaction of Slush Ice and Wind Waves".

In our present research, our major efforts during the past year have been Josberger's thesis study of the turbulent boundary layer adjacent to a vertical ice wall, and Martin and Kauffman's laboratory and theoretical study of wave damping by grease ice. We next describe in detail these two projects.

Melting of a vertical ice wall. Josberger's thesis on this subject is presently in draft form and is being read by the members of his reading committee. It should be available in report form early in 1979. The thesis consists of a discussion of his experiments on the melting of a vertical ice wall contained in warm seawater, the application of a numerical model to these experiments, and the results of his two iceberg cruises with the International Ice Patrol. In his experimental tank, the seawater temperature elevation above freezing ranged from 1 to 25 degrees, with most of his experiments in the range of 1-6 degrees. A turbulent boundary layer drives the melting; to parameterize the turbulence, he measures the wall melt rate, the wall temperature, and takes streak photographs of the flow. His detailed measurements give melt rate and wall temperature as a function of the far field temperature in both functional and graphical form. These relations will be useful as predictors of the melt rates of icebergs and pressure ridge keels.

Wave damping by grease ice. In the second set of experiments, Martin and Kauffman studied the interaction of surface waves with grease ice. These experiments took place in a tank measuring approximately 2 m long by 1 m wide, which is filled with seawater to a depth of 0.4 m. Using a wave generator located at one end of the tank to agitate the water, they grew layers of grease ice up to 0.3 m in thickness.

Within this grease ice, in a series of experiments they generated waves with periods between 0.4 to 0.6 seconds, or wavelengths of 0.25 to 0.54 m, at a variety of different amplitudes ranging from small to near-breaking. To observe the wave properties, they used a resistance probe placed at different stations down the tank to record the wave amplitude as a function of position in a series of approximately 40 experiments. They then used this information to develop a relation for how waves decay in grease ice.

The experiments showed that in all cases where the grease ice depth is greater than the depth of motion of the wave k^{-1} , where k is the wave number and k^{-1} was typically 40-100 mm in our experiments, that the wave amplitude decays linearly with the slope α . Further for a constant frequency as the wave amplitude at the paddle a_0 increased, α increased as a_0^2 , so that the wave damps out in a shorter distance as the amplitude increases. Second, we found over our range of frequencies that

$$\alpha = 0.24(a_0 k)^2 \quad (1)$$

where the wave number k follows from the dispersion relation

$$\sigma^2 = gk ,$$

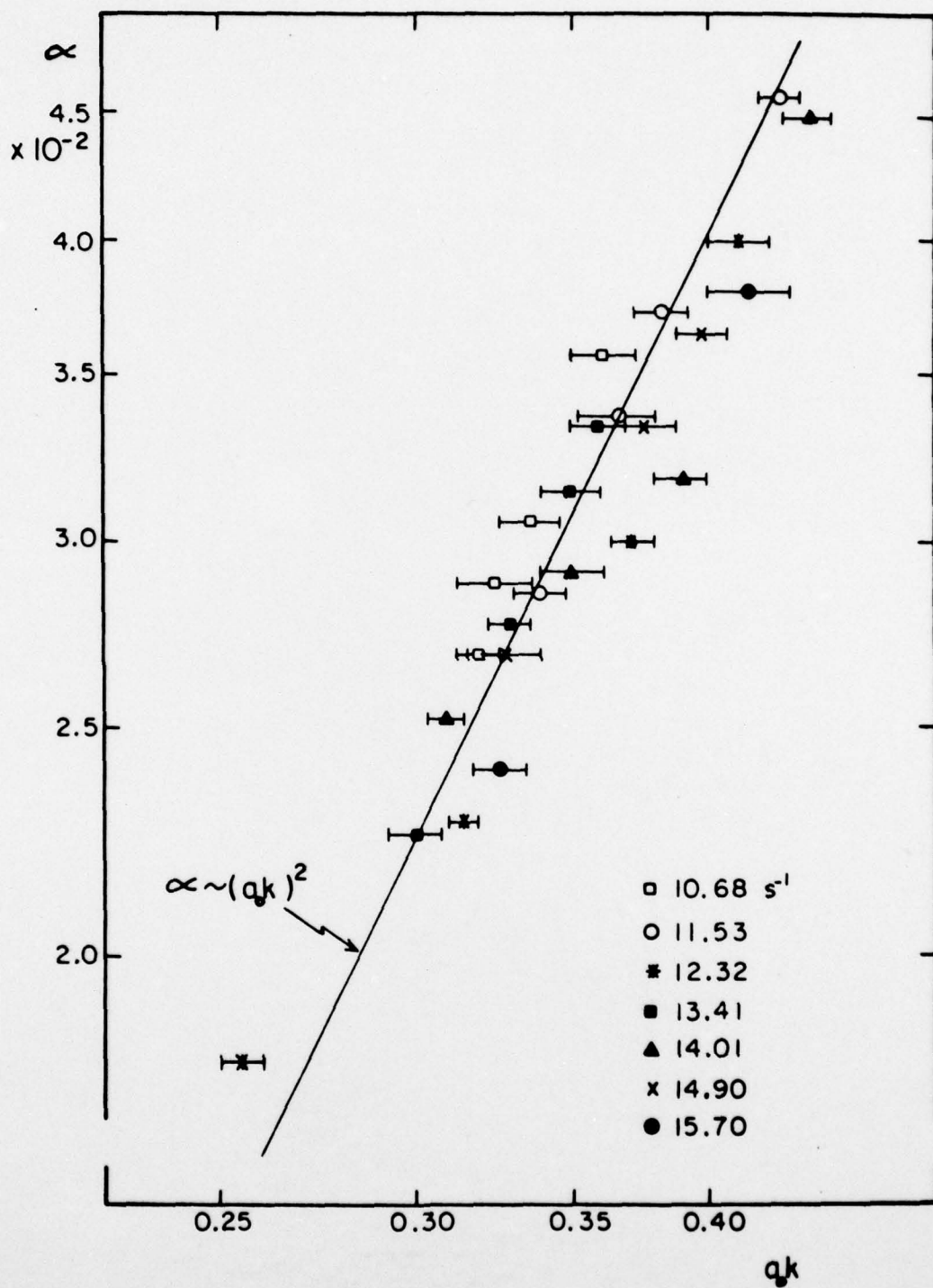
where g is the acceleration of gravity and σ is the wave frequency.

The attached figure compares on a log-log scale the data from 26 different runs with equation (1). The solid line shows (1) and the points represent different values of α plotted against $a_0 k$ at different frequencies. Examination of the figure shows that the data clusters around the line for

$0.20 < a_0 k < 0.45$. Because the maximum amplitude of any deep water wave cannot exceed $a_0 k = 0.45$, equation (1) may also be valid for the longer period wind-waves which occur at the ice edge.

The cause of this rapid linear wave decay is that the grease ice consists of a slurry of small ice platelets, measuring approximately 1 mm in diameter and 10 μm in thickness. At high shear rates, these platelets move independently. At low shear rates, the platelets sinter or pressure melt together into clusters, thus causing a viscosity increase and a linear decay. As the shear rate decreases further, the platelets form larger and larger clusters, until finally the grease ice ceases to behave as a liquid, but rather becomes an elastic solid so that the water waves propagate as elastic waves. Our present theoretical work centers on relating the above nonlinear viscosity to the observed wave properties. We are presently writing up this work for publication.

Finally, we have begun construction of a new wave tank measuring about 4 m long, 1 m deep, and 1.2 m wide. This tank, which should be completed by the end of December 1978, will be used to investigate wave decay in pancake ice.



Wave damping slope for grease ice versus wave amplitude times wave number. See text for further description.

REPORTS PUBLISHED AND IN PRESS

1. Grenfell, T. C. and G. A. Maykut, The optical properties of ice and snow in the Arctic Basin. Journal of Glaciology, 18, 80, 445-63, 1977.

Measurements of light transmission and reflection were carried out on first-year sea ice near Point Barrow, Alaska, and on multiyear ice near Fletcher's Ice Island in the Beaufort Sea (lat. 84°N, long. 77° W.). Spectral albedos (400-1000 nm) and extinction coefficients (400-800 nm) were determined for melt ponds, snow, and various types of bare ice. Albedos were largest in the 400-600 nm range, decreasing toward longer wavelengths at a rate which appeared to be related to the liquid-water content of the near-surface layers. Extinction coefficients remained nearly constant between 400 and 550 nm, but increased rapidly above 600 nm. At 500 nm, albedos ranged from 0.25 over mature melt ponds to 0.93 over dense dry snow, while the corresponding extinction coefficients ranged from 0.6 to 16 m⁻¹. Intensity profiles taken in the upper 50 cm of the ice indicated that the extinction coefficient at a particular wavelength was nearly constant with depth below 15 cm, although the bulk extinction coefficient decreased with depth because of the strong attenuation in the red. Near the surface it was found that multiyear ice absorbed slightly more energy than did first-year blue ice, but at depths below 10 cm the flux divergence in the first-year ice was three to four times larger than that in the multiyear ice. A simple procedure is described for estimating light transmission and absorption within the ice under clear or cloudy skies from total flux measurements at the surface. Methods by which satellite data could be used to estimate regional albedos, melt-pond fraction, and lead area are also presented.

2. Maykut, G. A., Energy exchange over young sea ice in the central Arctic. Journal of Geophysical Research, 83, 3646-58, 1978.

A simple model of heat transport through young sea ice is combined with climatological data on air temperatures and incoming radiation in the central Arctic to predict how each component of the surface heat balance is affected by changes in ice thickness. Results indicate that during the cold months the net heat input to the atmosphere from ice in the 0- to 0.4 m range is between 1 and 2 orders of magnitude larger than that from perennial ice. Once the ice exceeds a meter in thickness, there is little change in any of the heat fluxes as the ice thickens.

Although both the amount of absorbed shortwave radiation and the emitted longwave radiation depend on ice thickness, it is the turbulent fluxes which undergo the largest changes. The rate of heat exchange over thin ice is shown to be extremely sensitive to snow depth and assumed boundary layer temperatures. It is concluded that with the present ice thickness distribution in the central Arctic, total heat input to the atmospheric boundary layer from regions of young ice is equal to or greater than that from regions of open water or thick ice.

3. Maykut, G. A., On the heat and mass balance of the arctic ice pack.

Naval Research Reviews, 17-35, July 1978.

Dynamic and thermodynamic processes interact within the arctic ice pack to maintain a distribution of ice thickness which ranges continuously from open water to pressure ice tens of meters in thickness. Because of extremely large rates of ice growth and turbulent heat exchange in areas of open water and thin ice, such areas have the potential to make a significant contribution to the overall heat and mass balance of the ice pack. Field observations were combined with theoretical models of ice growth and thickness distribution to determine how thickness variations affected regional fluxes in the Central Arctic. The results show that the large-scale ice production, sensible and latent heat fluxes, salt input to the mixed layer, and absorption of shortwave radiation in the ocean are several times larger than would be expected with a uniform ice cover. This suggests that the interaction between atmosphere and ocean in the presence of a dynamic ice cover is much more vigorous than previously believed.

4. Josberger, Edward, A laboratory and field study of iceberg deterioration.

(In Hussieny, A. A., ed., Iceberg Utilization, Pergamon Press, London, 245-60) 1978.

Vertical ice walls in warm sea water deteriorate from the action of natural convective boundary layers. A cooperative field study with the International Ice Patrol shows that in 4°C seawater melt-driven upwelling occurs adjacent to an iceberg. The effects of the iceberg on the water column were to lower the temperature and salinity by 3.0°C and 0.5 ‰. In the laboratory this process was modeled using fresh water bubble-free ice sheets immersed in sodium chloride solutions of oceanic salinities and temperatures. The observed flow field next

to the ice face was laminar at the bottom, then went through a region of transition and finally became fully turbulent further up the ice. The length of the laminar layer for oceanic conditions has a maximum length of 0.5 m, at which point the saline Grashof number reaches a critical value 2×10^8 and the flow becomes turbulent. Measurements of the melt rate and the ice/water interface temperature in the turbulent regime show uniform temperatures and a melting rate that varies slowly in the vertical; this greatly facilitates theoretical modeling of the flow. For subpolar water temperatures, 0° to 5°C , the experiments show the melt rate to be of the order 0.1 m day^{-1} ; for tropical water temperatures, 25°C , the melt rate is of the order 2.5 m day^{-1} .

5. Martin, S., E. G. Josberger, and P. Kauffman, Wave-induced heat transfer to an iceberg. (In Hussieny, A. A., ed., Iceberg Utilization, Pergamon Press, London, 260-64) 1978.

This appendix compares field observations of wave-induced waterline erosion on icebergs with a laboratory experiment to show that the cause of the erosion is the heat carried to the ice by the Stokes drift.

6. Grenfell, T. C., The effects of ice thickness on the exchange of solar radiation over the polar oceans. Journal of Glaciology (in press).
7. Niedrauer, T., and S. Martin, Brine drainage features in young sea ice. Journal of Geophysical Research (in press).
8. Neshyba, S., and E. Josberger, An estimation of antarctic iceberg melt rates. Journal of Physical Oceanography (submitted).
9. Martin, S., A field study of brine drainage and oil entrainment in first-year sea ice. Journal of Glaciology (submitted).

SECURITY CLASSIFICATION OF THIS PAGE (When Data Entered)

REPORT DOCUMENTATION PAGE		READ INSTRUCTIONS BEFORE COMPLETING FORM
1. REPORT NUMBER ANNUAL REPORT NO. 10	2. GOVT ACCESSION NO.	3. RECIPIENT'S CATALOG NUMBER
4. TITLE (and Subtitle) ANNUAL REPORT NO. 10	5. TYPE OF REPORT & PERIOD COVERED INTERIM REPORT 1 OCT 77-30 SEPT 78	
	6. PERFORMING ORG. REPORT NUMBER	
7. AUTHOR(s) CONTRACT N00014-76-C-0234	8. CONTRACT OR GRANT NUMBER(s) N00014-76-C-0234	
9. PERFORMING ORGANIZATION NAME AND ADDRESS ARCTIC SEA AIR INTERACTION DEPARTMENT OF ATMOSPHERIC SCIENCES AK-40 UNIVERSITY OF WASHINGTON, SEATTLE, WA 98195	10. PROGRAM ELEMENT, PROJECT, TASK AREA & WORK UNIT NUMBERS NR 307-252	
11. CONTROLLING OFFICE NAME AND ADDRESS OFFICE OF NAVAL RESEARCH CODE 461, ARCTIC PROGRAM ARLINGTON, VA 22217	12. REPORT DATE 1 DECEMBER 1978	
	13. NUMBER OF PAGES 37	
14. MONITORING AGENCY NAME & ADDRESS (if different from Controlling Office)	15. SECURITY CLASS. (of this report) UNCLASSIFIED	
	15a. DECLASSIFICATION/DOWNGRADING SCHEDULE	
16. DISTRIBUTION STATEMENT (of this Report) THE DISTRIBUTION OF THIS REPORT IS UNLIMITED		
17. DISTRIBUTION STATEMENT (of the abstract entered in Block 20, if different from Report)		
18. SUPPLEMENTARY NOTES		
19. KEY WORDS (Continue on reverse side if necessary and identify by block number) ARCTIC OCEAN SEA ICE Sea Ice Desalination Light Scattering Surface Heat Balance Forecasting Optical Properties Grease Ice Thermodynamics Growth Thickness Distribution		
20. ABSTRACT (Continue on reverse side if necessary and identify by block number) The report summarizes research performed under Contract N00014-76-C-0234, NR 307-252, during the year 1 October 1977 - 30 September 1978. Research topics include: (i) growth and ablation of sea ice, (ii) light scattering and optical properties of sea ice, (iii) desalination of sea ice, (iv) thickness distribution of sea ice, (v) large-scale heat and mass balance in the central Arctic, (vi) ice forecasting, and (vii) formation of ice in a wave field.		

DD FORM 1473
1 JAN 73EDITION OF 1 NOV 68 IS OBSOLETE
S/N 0102-014-6601

SECURITY CLASSIFICATION OF THIS PAGE (When Data Entered)

DISTRIBUTION LIST

CONTRACT N00014-76-C-0234
NR 307-252

DR G LEONARD JOHNSON
CODE 461
OFFICE OF NAVAL RESEARCH
ARLINGTON, VA 22217

DEFENSE DOCUMENTATION CENTER
CAMERON STATION
ALEXANDRIA, VA 22314 (12 copies)

DIRECTOR, US NAVAL RESEARCH LAB
CODE 2627
WASHINGTON, DC 20375 (6 copies)

RESEARCH LIBRARY
NAVAL ELECTRONICS LAB CENTER
SAN DIEGO, CA 92152

COMMANDING OFFICER
CODE L61
NAVAL CIVIL ENGINEERING LAB
PORT HUENEME, CA 93043

DEPARTMENT OF THE ARMY
OFFICE, CHIEF OF ENGINEERS
ATTN DAEN-RDM
WASHINGTON, DC 20314

CHIEF OF ENGINEERS
ATTN DAEN-MCE-D
DEPARTMENT OF THE ARMY
WASHINGTON, DC 20314

COLD REGIONS RESEARCH & ENG LAB
PO BOX 282
HANOVER, NH 03755

DR REID A BRYSON
INST FOR ENVIRONMENTAL STUDIES
UNIVERSITY OF WISCONSIN
1225 W DAYTON STREET
MADISON, WI 53706

LIBRARIAN
NAVAL ARCTIC RESEARCH LAB
BARROW, AK 99723

WOODS HOLE OCEANOGRAPHIC INST
DOCUMENT LIBRARY LO-206
WOODS HOLE, MA 02543

RESIDENT REPRESENTATIVE
OFFICE OF NAVAL RESEARCH
UNIVERSITY OF WASHINGTON
3710 BROOKLYN AVE NE, UNIT 2
SEATTLE, WA 98105

DIRECTOR, INST OF POLAR STUDIES
OHIO STATE UNIVERSITY
125 SOUTH OVAL DRIVE
COLUMBUS, OH 43210

MR PAUL P LAUVER, PUBLICATIONS
ARCTIC INSTITUTE OF NORTH AMERICA
3426 NO WASHINGTON BLVD
ARLINGTON, VA 22201

COMMANDER
NAVAL UNDERSEA CENTER
ATTN TECHNICAL LIBRARY, CODE 1311
SAN DIEGO, CA 92132

DR KENNETH L HUNKINS
LAMONT-DOHERTY GEOLOGICAL OBSERVATORY
TORREY CLIFFE
PALISADES, NY 10964

SUPERINTENDENT
NAVAL POSTGRADUATE SCHOOL
LIBRARY CODE 2124
MONTEREY, CA 93940

DR E R POUNDER
RUTHERFORD PHYSICS BUILDING
MCGILL UNIVERSITY
3600 UNIVERSITY STREET
MONTREAL, PQ CANADA H3A 2T8

MR BEAUMONT BUCK
POLAR RESEARCH LABORATORY INC
123 SANTA BARBARA STREET
SANTA BARBARA, CA 93101

DR WARREN DENNER
NAVAL ARCTIC RESEARCH LABORATORY
BARROW, AK 99723

DR V P HESSLER
4230 EUTAW STREET
BOULDER, CO 80302

DISTRIBUTION LIST, CONTRACT N00014-76-C-0234, NR 307-252, Page 2

CHIEF OF NAVAL RESEARCH CODE 480D
OFFICE OF NAVAL RESEARCH
ARLINGTON, VA 22217

DR KOU KUSUNOKI
NATIONAL INSTITUTE OF POLAR RESEARCH
KAGA 1-9-10, ITABASHI-KU
TOKYO, JAPAN

CAPTAIN D C NUTT, USN (RET)
DEPARTMENT OF GEOGRAPHY
DARTMOUTH COLLEGE
HANOVER, NH 03755

DR T E ARMSTRONG
SCOTT POLAR RESEARCH INSTITUTE
CAMBRIDGE, CB2 1 ER
ENGLAND

MISS MOIRA DUNBAR
DEFENCE RESEARCH ESTABLISHMENT
OTTAWA, NATL DEFENCE HEADQUARTERS
OTTAWA, ONTARIO K1A 0Z4, CANADA

DR A R MILNE
DEFENCE RESEARCH ESTABL PACIFIC
FLEET MAIL OFFICE
VICTORIA, B.C., CANADA

DR SVENN ORVIG
MCGILL UNIVERSITY
DEPT OF METEOROLOGY
PO BOX 6070
MONTREAL 101, QUEBEC, CANADA

DEPARTMENTAL LIBRARY-SERIALS
DEPARTMENT OF THE ENVIRONMENT
OTTAWA, CANADA K1A 0H3

DR K M RAE
VICE PRESIDENT FOR RESEARCH
UNIVERSITY OF ALASKA
FAIRBANKS, AK 99701

DR ROBERT L RAUSCH
DEPARTMENT OF MICROBIOLOGY
WESTERN COLLEGE OF VET MEDICINE
UNIVERSITY OF SASKATCHEWAN
SASKATOON, SASKATCHEWAN, CANADA
S7N 0W0

THE LIBRARIAN
SCOTT POLAR RESEARCH INSTITUTE
CAMBRIDGE CB2 1ER, ENGLAND

DR GEORGE A LLANO
ACTING CHIEF SCIENTIST
OFFICE OF POLAR PROGRAMS
NATIONAL SCIENCE FOUNDATION
WASHINGTON, DC 20550

DR MICHAEL KELLY
SCHOOL OF ENVIRONMENTAL SCIENCES
UNIVERSITY OF EAST ANGLIA
NORWICH NR4 7TJ ENGLAND

MR LOUIS DEGOES
EXECUTIVE SECRETARY
POLAR RESEARCH BOARD
NATIONAL ACADEMY OF SCIENCES
2101 CONSTITUTION AVENUE, NW
WASHINGTON, DC 20418

DR HARLEY J WALKER
DEPARTMENT OF GEOGRAPHY
LOUISIANA STATE UNIVERSITY
BATON ROUGE, LA 70803

DR JOHN C F TEDROW
DEPARTMENT OF SOILS, LIPMAN HALL
RUTGERS UNIVERSITY
NEW BRUNSWICK, NJ 08903

MR M M KLEINERMAN
PROJECT MANAGER FOR ARCTIC ASW
US NAVAL ORDNANCE LABORATORY
WHITE OAK, MD 20910

MR M R HERRMAN
NAVAL FACILITIES ENGINEERING COMMAND
CODE 032A, YARDS & DOCKS ANNEX ROOM 2B1
WASHINGTON, DC 20390

NORSK POLARINSTITUTT
ROLFSTANGVN 12, POSTBOKS 158
1330 OSLO LUFTHAVN, NORWAY

LIBRARIAN (CODE 8160)
US NAVAL OCEANOGRAPHIC OFFICE
NSTL STATION
BAY ST. LOUIS, MS 39522

DISTRIBUTION LIST, CONTRACT N00014-76-C-0234, NR 307-252, Page 3

PROF WILLIAM MCINTIRE
COASTAL STUDIES INSTITUTE
LOUISIANA STATE UNIVERSITY
BATON ROUGE, LA 70803

DR CHARLES E BEHLKE, DIRECTOR
INST OF ARCTIC ENVIRONMENTAL ENGINEERING
UNIVERSITY OF ALASKA
COLLEGE, AK 99701

DR W M SACKINGER
DEPT OF ELECTRICAL ENG
UNIVERSITY OF ALASKA
FAIRBANKS, AK 99701

WORLD DATA CENTER: A FOR GLACIOLOGY
INST OF ARCTIC & ALPINE RESEARCH
UNIVERSITY OF COLORADO
BOULDER, CO 80309

MANAGER, INUVIK RESEARCH LAB
BOX 1430
INUVIK, NW TERRITORIES XOE OT0
CANADA

METEOROLOGICAL OFFICE LIBRARY
LONDON ROAD
BRACKNELL, BERKSHIRE, ENGLAND

DR WESTON BLAKE, JR.
GEOLOGICAL SURVEY OF CANADA
DEPT OF ENERGY, MINES & RESOURCES
601 BOOTH STREET
OTTAWA, ONTARIO K1A 0E8, CANADA

PROF DR ALEXSANDER KOSIBA
KATEFRA I OBSERWATORIUM
METEOROLOGI I KLIMATOLOGII
UNIwersytetu WROCLAWSKIEGO
WROCLAW 9, U..CMENTARNA 8,
POLAND

CHIEF OF NAVAL RESEARCH
OFFICE OF NAVAL RESEARCH CODE 412
ARLINGTON, VA 22217

CENTRE NATIONAL DE LA RECHERCHE SCIENTIFIQUE
LABORATOIRE DE GLACIOLOGIE
UNIVERSITE DE GRENOBLE 1
SERVICE DE GEOPHYSIQUE
2, RUE TRES-CLOITRES
38-GRENOBLE, FRANCE

CHIEF OF NAVAL RESEARCH
OFFICE OF NAVAL RESEARCH CODE 414
ARLINGTON, VA 22217

CENTRE D'ETUDES ARCTIQUES
ECOLE PRATIQUE DES HAUTES ETUDES
VI SECTION (SORBONNE)
6, RUE DE TOURNON
PARIS-6, FRANCE

NATIONAL INST OF OCEANOGRAPHY
WORMLEY, GODALMING
SURREY, ENGLAND

DR ING O MAGGIOLO
FACULTAD DE INGENIERIA
HERRERA Y REISSIG 585
MONTEVIDEO, URUGUAY

STOCKHOLMS UNIVERSITET
NATURGEOGRAFISKA INSTITUTIONEN
BOX 6801
113 86 STOCKHOLM, SWEDEN

MRS GAIL HORWOOD
METEOROLOGY LIBRARY
MCGILL UNIVERSITY
MONTREAL, QUEBEC, CANADA

DR E L LEWIS
FROZEN SEA RESEARCH GROUP
INSTITUTE OF OCEAN SCIENCES
9860 W SAANICH ROAD
SIDNEY B.C. CANADA V8L-3S2

LIBRARIAN, TECH LIBRARY DIV
NAVAL CIVIL ENG LABORATORY
PORT HUENEME, CA 93041

CONTRACT ADMINISTRATOR
OFFICE OF NAVAL RESEARCH BR OFFICE
1030 EAST GREEN STREET
PASADENA, CA 91106

DISTRIBUTION LIST, CONTRACT N00014-76-C-0234, NR 307-252, Page 4

POLAR INFORMATION SERVICE
OFFICE OF POLAR PROGRAMS
NATIONAL SCIENCE FOUNDATION
WASHINGTON, DC 20550

PROF RICHARD S TANKIN
DEPT OF MECHANICAL ENGINEERING
NORTHWESTERN UNIVERSITY
EVANSTON, IL 60201

DR DONALD W HOOD
INSTITUTE FOR MARINE SCIENCE
UNIVERSITY OF ALASKA
FAIRBANKS, AK 99701

DR LAWRENCE COACHMAN
DEPARTMENT OF OCEANOGRAPHY
UNIVERSITY OF WASHINGTON
SEATTLE, WA 98195

MARINE SCIENCES CENTRE LIBRARY
MCGILL UNIVERSITY
PO BOX 6070
MONTREAL, PQ, CANADA H3A 2T8

DR T SAUNDERS ENGLISH
DEPARTMENT OF OCEANOGRAPHY
UNIVERSITY OF WASHINGTON
SEATTLE, WA 98195

DR DAVID CLARK
DEPARTMENT OF GEOLOGY
UNIVERSITY OF WISCONSIN
MADISON, WI 53706

DR KNUT AAGARD
DEPARTMENT OF OCEANOGRAPHY
UNIVERSITY OF WASHINGTON
SEATTLE, WA 98195

DR ARTHUR LACHENBRUCH
BRANCH OF GEOPHYSICS
US GEOLOGICAL SURVEY
345 MIDDLEFIELD ROAD
MENLO PARK, CA 94025

DEFENCE RESEARCH BOARD
DEPT OF NATIONAL DEFENCE
190 O'CONNOR STREET
OTTAWA, ONTARIO, CANADA K1A 0Z3

DR KEITH MATHER
GEOPHYSICAL INSTITUTE
UNIVERSITY OF ALASKA
COLLEGE, AK 99701

DR ALBERT H JACKMAN
CHAIRMAN DEPT OF GEOGRAPHY
WESTERN MICHIGAN UNIVERSITY
KALAMAZOO, MI 49001

MR ROBERT D KETCHUM JR
BLDG 70, CODE 8050
NAVAL RESEARCH LAB
WASHINGTON, DC 20390

DR GUNTER WELLER
GEOPHYSICAL INSTITUTE
UNIVERSITY OF ALASKA
COLLEGE, AK 99701